Low-Complexity Channel Estimation Algorithm for MIMO-OFDM Systems

Ali Beydoun, Hamzé H. Alaeddine

Abstract—One of the main challenges in MIMO-OFDM system to achieve the expected performances in terms of data rate and robustness against multi-path fading channels is the channel estimation. Several methods were proposed in the literature based on either least square (LS) or minimum mean squared error (MMSE) estimators. These methods present high implementation complexity as they require the inversion of large matrices. In order to overcome this problem and to reduce the complexity, this paper presents a solution that benefits from the use of the STBC encoder and transforms the channel estimation process into a set of simple linear operations. The proposed method is evaluated via simulation in AWGN-Rayleigh fading channel. Simulation results show a maximum reduction of 6.85% of the bit error rate (BER) compared to the one obtained with the ideal case where the receiver has a perfect knowledge of the channel.

Keywords—Channel estimation, MIMO, OFDM, STBC, CAZAC sequence.

I. INTRODUCTION

THE combination of MIMO (Multiple Input Multiple Output) with OFDM (Orthogonal Frequency Division Multiplexing) is a key solution for the future generation of wireless communication system to achieve the exponential increase in the data rate [1]. This is due to its simple implementation, high spectral efficiency, reliability and robustness against frequency-selective fading channels. Indeed, OFDM divides the entire frequency selective fading channel into many narrow flat parallel subchannels using overlapped orthogonal subcarries which thereby reduces Inter-Symbol Interference (ISI) and increases the spectrum efficiency. Moreover, the reliability is increased by exploiting diversity of the MIMO system using Space Time Block Code (STBC) without increasing the transmitted power [2]. However, the major challenge faced in MIMO-OFDM systems is the estimation of the Channel State Information (CSI) at the receiver side in order to recover the transmitted data correctly and maintain the expected performance of the system [3]. The estimator precision directly affects the overall performance of MIMO-OFDM system [4]. Several approaches for channel estimation have been proposed in the literature. Blind channel estimator, based on the second-order statistics of the received signals, shows good performances [3]. However, this technique is limited to slow time varying channels as it requires a long data record and has high computational complexity. On the other hand, pilot aided channel estimators using pilot tones, that are known a priori to the receiver, multiplexed along with

A. Beydoun and H. Alaeddine are with the Department of Physics, Lebanese University, Beirut, Lebanon, (e-mail: ali.beydoun@ul.edu.lb, hamze.alaeddine@ul.edu.lb)

the data stream are simple to implement and can be applied to different types of channels [5]. It is important to note that the use of pilots can slightly affect the useful data rate. There are two types of pilot arrangements:

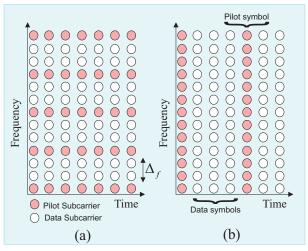


Fig. 1 (a) Block-type pilot arrangement, (b) Comb-type pilot arrangement

- Comb-Type where pilots are uniformly distributed within each OFDM symbol with a specific period of frequency bins Δ_f (Fig.1 (a)) [4]. At the receiver side, an estimation algorithm is used to estimate the channel frequency response at the pilot subcarriers. Then, an interpolation in the frequency domain is applied to estimate the channel frequency response at the data subcarriers. Therefore, the interpolation error is inevitably introduced. Different interpolation techniques were proposed in the literature:
 - Linear interpolation estimates the channel response at data subcarriers from the equation of a straight line connecting the channel response at two pilot subcarriers.
 - Low pass interpolation is performed by inserting zeros between two consecutive channel response estimated at two pilot subcarriers and then applying a lowpass FIR filter to estimate the channel response at data subcarriers.
 - Spline cubic interpolation gives the best estimate of channel response with a smooth frequency response in the whole bandwidth at the cost of high complexity.

The selection of an interpolation technique is a compromise between interpolation error and complexity.

The number of pilots must be as minimum as possible in order to maintain high data transmission efficiency. However, in fast fading selective channel, where the number of paths between i^{th} transmit antenna and j^{th} receive antenna is high, the distance between pilots must be decreased in order to obtain an accurate estimation of the channel frequency response according to Shanon theorem. Consequently, increasing the number of pilot subcarriers would introduce prohibitive reduction in the data rate and therefore leads to an inefficient use of the bandwidth.

• Block-Type where pilot tones are inserted into all frequency bins within periodic intervals of OFDM blocks(Fig.1 (b)) [4]. It has been shown in [6] that block type has better performance than comb type in fast fading channel.

For both types, the estimation of the channel at pilot frequencies is performed using either least square (LS) or minimum mean squared error (MMSE) estimators. MMSE estimator has better performance at the cost of high complexity as it requires the inversion of large matrices. In order to reduce the channel estimation complexity, the aim of this paper is to present AN estimation technique taking advantage of the use of the STBC encoder to transform the estimation process into a simple linear operation.

The rest of the paper is organized as follows. Section II introduces briefly the MIMO-OFDM system model. The proposed channel estimation algorithm is described in Section III. Simulations results and comparison are discussed in Section IV. Finally, the conclusion is drawn in Section V.

II. MIMO-OFDM SYSTEM MODEL

A simple 2×2 MIMO-OFDM system with two transmit antennas and two receive antennas using the STBC-Alamouti encoder is shown in Fig. 2. The binary data to be transmitted is first mapped to the complex modulation symbols by using M-QAM signal constellation. The QAM symbols are then multiplexed with pilot symbols used in the channel estimation (see Section III). Afterwards, the resulting symbols are fed to the STBC encoder (Space-Time Block Coding) allowing to exploit the spatial diversity and to increase the reliability of transmission with the codeword matrix illustrated in Table I [7].

 $\begin{tabular}{l} TABLE\ I\\ ENCODED\ DATA\ ACCORDING\ TO\ TIME\ AND\ SUBCARRIER \end{tabular}$

| Subcarrier index | Antenna 1 | Antenna 2 |
|--------------------|--------------------------|-------------------------|
| Even index $(2k)$ | $S_1[2k]$ | $S_2[2k]$ |
| Odd index $(2k+1)$ | $S_1[2k+1] = -S_2^*[2k]$ | $S_2[2k+1] = S_1^*[2k]$ |

Then, the encoder outputs pass through a serial to parallel converters to generate two frames X_1 and X_2 of N samples at the input of the IFFT blocks:

$$X_1 = (S[0] - S^*[1]S[2] - S^*[3] \cdot \dots - S^*[N-1])$$
 (1)

$$X_2 = (S[1] S^*[0] S[3] S^*[2] \cdots S^*[N-2])$$
 (2)

Next, the Inverse Fast Fourier Transform (IFFT) is applied to generate the OFDM symbols x_1 and x_2 in the time domain. A cyclic prefix (CP), the replica of last part of the OFDM symbol, is attached at the beginning of each time domain OFDM symbol to preserve the orthogonality between subcarriers and to eliminate interference between the adjacent OFDM symbols. The length of CP should exceed the maximum excess delay of the multipath propagation channel [8]. After the insertion of CP, the resultant OFDM symbols are first converted to serial form and then multiplexed with preamble sequences for the timing synchronization before to be transmitted simultaneously over the 2×2 AWGN Rayleigh channel. The OFDM symbol transmitted from the j^{th} antenna is given by [8]:

$$x_{j}(n) = \frac{1}{\sqrt{N}} \sum_{k=0}^{N} X_{j}(k) e^{j\frac{2\pi nk}{N}}$$
 (3)

where $X_j(k)$ is the transmitted symbol in the frequency domain before the IFFT and N is the number of sub-carriers for one OFDM symbol. The Rayleigh channel between i^{th} receive antenna and j^{th} transmit antenna is given by:

$$h_{ij}(t) = \sum_{l=0}^{L} \alpha_{ij}^{l} \delta\left(t - \tau_{ij}^{l}\right) \tag{4}$$

where L is the number of multi-path channels between i^{th} receiver and j^{th} transmitter. α_{ij}^l denotes the channel gain and τ_{ij}^l denotes the delay of the path. The received signal r_i , on each receive antenna R_i , is the convolution of the channel impulse response and the transmitted signal and is given by:

$$r_i(t) = \sum_{j=1}^{2} \sum_{l=0}^{L} \left(\alpha_{ij}^l \delta \left(t - \tau_{ij}^l \right) * t_j(t) \right) + n_i(t), \ i = 1, 2$$
 (5)

where t_j is the transmitted signal on the transmit antenna T_j , n_i is the additive white Gaussian noise (AWGN).

At the receiver side, the first block, after the analog to digital converter (ADC), is the timing synchronization block in order to detect the beginning of OFDM symbols and ensure correct demodulation. A new fast algorithm for this purpose was proposed in [9]. After a good timing synchronization, the cyclic prefix of each OFDM symbol is removed. Then, the signal returns back into frequency domain thanks to the FFT block. It is important to note that, if the cyclic prefix length is higher than or equal the number of multipaths (L) of the 2×2 AWGN Rayleigh channel, the linear convolution of the transmitted signal with the channel impulse response is converted into circular convolution and therefore the FFT output can be expressed as:

$$Y_i(k) = \sum_{j=1}^{N_t=2} X_j(k) H_{ij}(k) + N_i(k) \quad i = 1, 2$$
 (6)

where Y_i is the received signal, X_j the transmitted symbol, H_{ij} is the frequency response of the channel between i^{th} receive antenna and j^{th} transmit antenna on the k^{th} subcarrier of the OFDM symbol, and N_i is the additive complex Gaussian noise with zero mean and variance σ_N^2 .

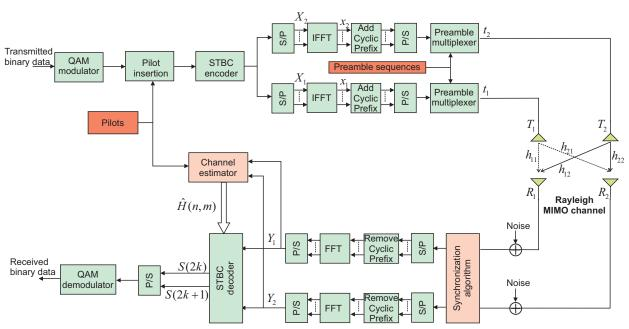


Fig. 2 Simplified block diagram of MIMO-OFDM system

The FFT outputs are first converted into serial and then sent to the STBC decoder that estimates the transmitted OFDM symbols using the channel state information delivered by the channel estimator. Based on the assumption that the channel frequency response remains approximately constant over two adjacent (odd and even) subcarriers (see section III):

$$H_{ij}(2k) = H_{ij}(2k+1) \tag{7}$$

the estimated even and odd symbols by the STBC decoder are given by (see appendix A):

$$\tilde{S}(2k) = \frac{\sum_{i=1}^{2} H_{i1}^{*}(2k) Y_{i}(2k) + H_{i2}(2k) Y_{i}^{*}(2k+1)}{\sum_{i=1}^{2} \sum_{j=1}^{2} \|H_{ij}(2k)\|^{2}}$$
(8)

$$\tilde{S}(2k+1) = \frac{\sum_{i=1}^{2} H_{i2}^{*}(2k) Y_{i}(2k) - H_{i1}(2k) Y_{i}^{*}(2k+1)}{\sum_{i=1}^{2} \sum_{j=1}^{2} \|H_{ij}(2k)\|^{2}}$$

After that, a Maximum Likelihood detector is used to associate the estimated values to the nearest symbols in the QAM constellation. Finally, a QAM demodulator is used to demodulate and recover the binary data.

III. PROPOSED CHANNEL ESTIMATION SCHEME

In order to reduce the complexity and to avoid the interpolation error, the proposed channel estimation algorithm is based on block type arrangement. It consists to inserts pilot symbol between OFDM data symbols in periodic intervals of

OFDM blocks. The pilot symbol, known by the receiver, is given by:

$$P = [P(0)P(1)P(2)\cdots P(N-1)]$$
 (10)

It can be composed of either CAZAC sequences [10] or constant amplitude complex number on all subcarriers. After applying the STBC encoder, the inputs of the IFFT blocks are given by:

$$X_1 = [P(0) - P^*(1) \cdots P(2k) - P^*(2k+1) \cdots - P^*(N-1)]$$
(11)

$$X_2 = [P(1)P^*(0)\cdots P(2k+1)P^*(2k)\cdots P^*(N-2)]$$
(12)

As the method is based on STBC, channel parameters have been assumed constant over two adjacent subcarriers (7). Therefore, at the receiver side, the output of the FFT block (6) in the first branch at two adjacent subcarriers can be expressed by the following matrix form:

$$\begin{bmatrix} Y_{1}(2k) \\ Y_{1}(2k+1) \end{bmatrix} = \begin{bmatrix} P(2k) & P(2k+1) \\ -P^{*}(2k+1) & P^{*}(2k) \end{bmatrix} \begin{bmatrix} H_{11}(2k) \\ H_{12}(2k) \end{bmatrix} + \begin{bmatrix} N_{1}(2k) \\ N_{2}(2k+1) \end{bmatrix}$$
(13)

Then multiplying both sides of 13 by the matrix:

$$\begin{bmatrix}
P^*(2k) & -P(2k+1) \\
P^*(2k+1) & P(2k)
\end{bmatrix}$$
(14)

The resulting equation is:

$$\begin{bmatrix} P^{*}(2k) & -P(2k+1) \\ P^{*}(2k+1) & P(2k) \end{bmatrix} \begin{bmatrix} Y_{1}(2k) \\ Y_{1}(2k+1) \end{bmatrix} = \\ \left(\|P(2k)\|^{2} + \|P(2k+1)\|^{2} \right) & H_{11}(2k) \\ H_{12}(2k) \end{bmatrix} + \\ \underbrace{\begin{bmatrix} P^{*}(2k) & -P(2k+1) \\ P^{*}(2k+1) & P(2k) \end{bmatrix}}_{Noise} \begin{bmatrix} N_{1}(2k) \\ N_{2}(2k+1) \end{bmatrix} +$$
(15)

The first row of 15 gives:

$$H_{11}(2k) = \frac{P^*(2k)Y_1(2k) - P(2k+1)Y_1(2k+1)}{\|P(2k)\|^2 + \|P(2k+1)\|^2} + \frac{P^*(2k)Y_1(2k) - P(2k+1)}{\|P(2k+1)\|^2} + \frac{P^*(2k+1)}{\|P(2k+1)\|^2} + \frac{P^*(2k+1$$

$$\underbrace{\frac{P^*(2k)N_1(2k) - P(2k+1)N_2(2k+1)}{\|P(2k)\|^2 + \|P(2k+1)\|^2}_{Error}}_{(16)}$$

Therefore, the channel parameters can be estimated by:

$$\hat{H}_{11}(2k) = \frac{P^*(2k)Y_1(2k) - P(2k+1)Y_1(2k+1)}{\|P(2k)\|^2 + \|P(2k+1)\|^2}$$
(17)

$$\hat{H}_{12}(2k) = \frac{P^*(2k+1)Y_1(2k) + P(2k)Y_1(2k+1)}{\|P(2k)\|^2 + \|P(2k+1)\|^2}$$
(18)

In the same way, the other channel parameters can be estimated using the output Y_2 in the second branch:

$$\hat{H}_{21}(2k) = \frac{P^*(2k)Y_2(2k) - P(2k+1)Y_2(2k+1)}{\|P(2k)\|^2 + \|P(2k+1)\|^2}$$
(19)

$$\hat{H}_{22}(2k) = \frac{P^*(2k+1)Y_2(2k) + P(2k)Y_2(2k+1)}{\|P(2k)\|^2 + \|P(2k+1)\|^2}$$
 (20)

It is important to note that due to the orthogonality in the STBC encoder, the channel parameters are estimated using simple linear operation instead of large matrices inversion required in Ls and MMSE algorithms. Thus, the implementation complexity is considerably reduced. Moreover, it is clear, from 17, 18, 19 and 20, that the estimation error can be reduced significantly by increasing the pilot's amplitude. However, the amplitude of the pilots is limited by the power amplifier in order to stay in the linear operating region and avoid any kind of non linearities that generate interference on the adjacent OFDM bands [11].

IV. SIMULATION RESULTS

The performance of the proposed channel estimation algorithm is evaluated by computer simulations using MATLAB. MIMO-OFDM system parameters used in the simulation are indicated in table II. We assume that a perfect synchronization is performed before applying the channel estimation algorithm [9]. Moreover, the cyclic prefix length is chosen to be greater than the maximum delay spread in order to avoid inter-symbol interference. Simulations are carried out for different signal to noise ratios (SNR). Each BER value is estimated using an average of 100 independent Monte Carlo trials.

TABLE II SIMULATION PARAMETERS

| Parameter | Value |
|------------------------------|------------------------------|
| Number of transmit antennas | 2 |
| Number of receive antennas | 2 |
| FFT/IFFT length | N |
| Cyclic Prefix length | 16 |
| Modulation tecnique | QAM |
| Channel bandwidth | 20 Mz |
| Channel type [12] | Multi-path Rayleigh and AWGN |
| Pilot type | CAZAC |
| Number of channel multi-path | L |

Fig. 3 shows the module of the transmitted signals by the two antennas over short period of time. The pilot symbols module, repeated every 20 OFDM symbols, is constant as pilot symbols are based on CAZAC sequences that conserve constant amplitude in the time domain.

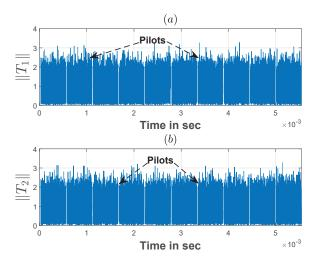


Fig. 3 Module of the transmitted signals over the two antennas T_1 and T_2

The module of the four estimated channels at different pilot symbols with an SNR=20dB is shown in Fig. 4. In addition, Fig. 5 presents the ideal and the estimated channel frequency response from one pilot symbol. It can be clearly noticed that there is a small difference between the ideal curve and the estimated one. This difference will have a direct impact on the BER.

After applying the channel estimation algorithm, the constellation of the received symbols over AWGN Rayleigh channel with $L=6,\,N=512$ and SNR=20dB is presented in Fig. 6.

Fig. 7 shows the bit error rate with respect to the SNR for different OFDM symbol size N. It can be noticed that for low SNR ($\leq 10dB$), the performance is determined by the AWGN level that dominates the channel estimation noise. However, for large SNR, it can be shown that the higher the OFDM symbol size is, the lower the BER. Indeed, increasing the OFDM symbol size will divide the whole channel bandwidth into smaller subcarriers bandwidth and consequently reduces the estimation error. It can be observed also that from an OFDM symbol size of 512, there will be no more significant

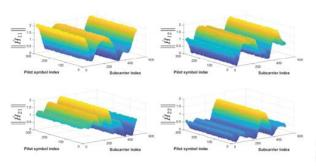


Fig. 4 Evolution of the estimated channel frequency reponse over all pilot symbols for all channels

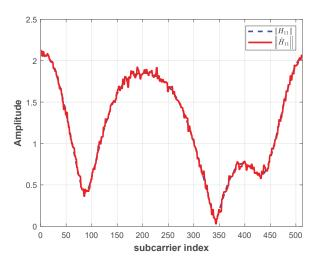


Fig. 5 Difference between the ideal and the estimated channel frequency response for the channel ${\cal H}_{11}$

improvement in the BER.

The impact of QAM constellation size is shown in Fig. 8. It can be observed that increasing the constellation size will reduce the distance between symbols and thus increase the BER.

Figs. 9 and 10 show the BER with respect to the SNR for different channel lengths with OFDM symbol size of 512 and 64 respectively. It can be shown that with high OFDM symbol size (N=512), the channel estimation algorithm performs well regardless the length of the Rayleigh channel L. However, with low OFDM symbol size (N=64) and large SNR $(\geq 14dB)$, the higher the length of the channel is, the higher the BER. In fact, increasing the channel length L creates fast variations in the channel frequency response and therefore an FFT size of 64 is not enough to have a good representation of the channel frequency response according to Shanon theorem. On the other hand, with smooth channel frequency response (L=2), an OFDM symbol size of 64 could be enough to obtain good estimation of the channel frequency response.

Fig. 11 presents a comparison between the BER obtained with the proposed algorithm and the one obtained in the ideal case where it is assumed that a perfect channel knowledge is known at the receiver side. It can be noticed that the BER

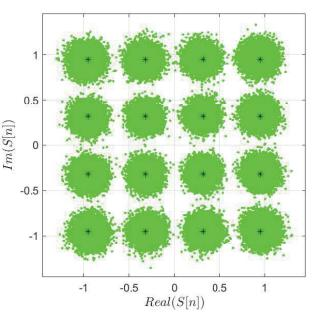


Fig. 6 Symbol dispersion at the output of the STBC decoder with $L=6,\ N=512$ and SNR=20dB

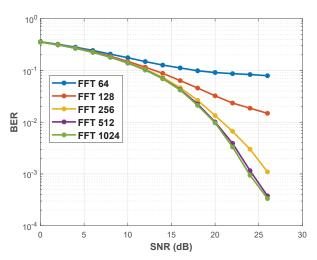


Fig. 7 BER for different FFT size N with QAM=64 and L=6

reaches a maximum reduction of 6.85% at SNR=25dB due the estimation error.

In order to characterize the variation of the expected performance, Fig. 12 shows the relative frequency distribution of the BER with 10000 independent Monte Carlo trials with $QAM=4,\ N=512,\ L=6$ and SNR=10dB. It can be shown that, with the proposed channel estimation algorithm, the relative frequency distribution of the BER presents an increase of 15.5% on the mean and 2.46% on the variance compared to the values obtained with the ideal channel.

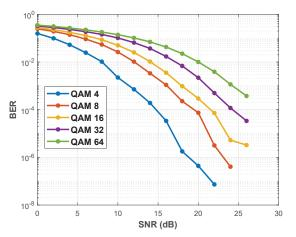


Fig. 8 BER for different QAM size with FFT size N=512 and channel length $L=6\,$

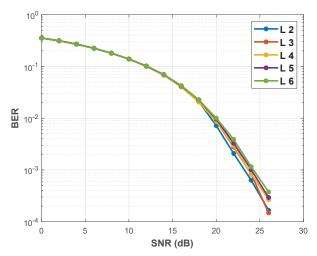


Fig. 9 BER for different channel length L with FFT size N=512 and $QAM=64\,$

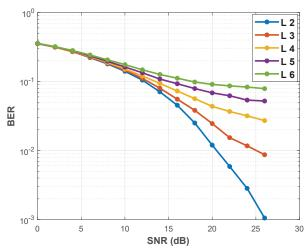


Fig. 10 BER for different channel length L with FFT size N=64 and $QAM=64\,$

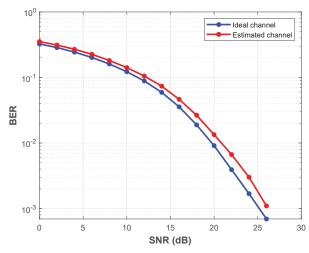


Fig. 11 BER with respect to the SNR obtained with ideal and estimated channel with the following parameters: $QAM=64,\ N=256$ and L=6

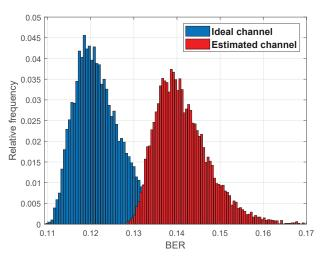


Fig. 12 Relative frequency distribution of the BER with ideal and estimated channel resulting from 10000 Monte Carlo trials with QAM=64, $N=256,\,SNR=10dB$ and L=6

V. CONCLUSION

efficient channel estimation algorithm MIMO-OFDM system has been proposed in this paper. A theoretical derivation of the channel estimator has been conducted. The proposed algorithm reduces considerably the implementation complexity compared to the most popular LS and MMSE algorithms that require large matrix inversion. Indeed, the channel estimation process is reduced to a simple linear operation due to the orthogonality between adjacent symbols provided by the STBC encoder. Moreover, the proposed algorithm is based on block type pilots which eliminates the need of interpolation technique and therefore removes the resulting interpolation error. The proposed algorithm shows satisfactory performance with an increase of 15.5% on the mean and 2.46% on the variance of the

relative frequency distribution of the BER compared to the values obtained with the ideal channel parameters. Finally, It

is important to mention that this method could be extended without any loss of generality to higher order MIMO systems.

APPENDIX A

Proof of equations 8 and 9

The output of the FFT algorithm at adjacent subcarriers in both channels are given by the following equations:

$$Y_1(2k) = H_{11}(2k) S(2k) + H_{12}(2k) S(2k+1) + N_1(2k)$$
(21)

$$Y_1(2k+1) = -H_{11}(2k+1)S^*(2k+1) + H_{12}(2k+1)S^*(2k) + N_1(2k+1)$$
(22)

$$Y_2(2k) = H_{21}(2k) S(2k) + H_{22}(2k) S(2k+1) + N_2(2k)$$
(23)

$$Y_2(2k+1) = -H_{21}(2k+1)S^*(2k+1) + H_{22}(2k+1)S^*(2k) + N_2(2k+1)$$
(24)

The STBC decoder combines the FFT outputs according to the following equations:

$$C(2k) = H_{11}^{*}(2k)Y_{1}(2k) + H_{12}(2k+1)Y_{1}^{*}(2k+1) + H_{21}^{*}(2k)Y_{2}(2k) + H_{22}(2k+1)Y_{2}^{*}(2k+1)$$
(25)

$$C(2k+1) = H_{12}^{*}(2k) Y_{1}(2k) - H_{11}(2k+1) Y_{1}^{*}(2k+1) + H_{22}^{*}(2k) Y_{2}(2k) - H_{21}(2k+1) Y_{2}^{*}(2k+1)$$
(26)

By substituting 21,22, 23, 24 into 25 we obtain:

$$C(2k) = \|H_{11}(2k)\|^{2} S(2k) + H_{11}^{*}(2k)H_{12}(2k)S(2k+1) + H_{11}(2k)N_{1}(2k) -H_{12}(2k+1)H_{11}^{*}(2k+1)S(2k+1) + \|H_{12}(2k+1)\|^{2} S(2k) + H_{12}^{*}(2k+1)N_{1}(2k+1) + \|H_{21}(2k)\|^{2} S(2k) + H_{21}^{*}(2k)H_{22}(2k)S(2k+1) + H_{21}^{*}(2k)N_{2}(2k) -H_{22}(2k+1)H_{21}^{*}(2k+1)S(2k+1) + \|H_{22}(2k+1)\|^{2} S(2k) + H_{21}^{*}(2k)N_{2}(2k+1)$$

$$(27)$$

Assuming that $H_{ij}(2k) = H_{ij}(2k+1)$, 27 can be simplified into the following form:

$$C(2k) = \left(\sum_{i=1}^{2} \sum_{j=1}^{2} \|H_{ij}(2k)\|^{2}\right) S(2k) + \underbrace{H_{11}^{*}(2k)N_{1}(2k) + H_{12}(2k)N_{1}^{*}(2k+1) + H_{21}^{*}(2k)N_{2}(2k) + H_{22}(2k)N_{2}^{*}(2k+1)}_{Noise}$$
(28)

And therefore an estimation of the received symbol on even subcarriers is given by:

$$\tilde{S}(2k) \approx \frac{C(2k)}{\sum_{i=1}^{2} \sum_{j=1}^{2} \|H_{ij}(2k)\|^{2}} = \frac{\sum_{i=1}^{2} H_{i1}^{*}(2k) Y_{i}(2k) + H_{i2}(2k) Y_{i}^{*}(2k+1)}{\sum_{i=1}^{2} \sum_{j=1}^{2} \|H_{ij}(2k)\|^{2}}$$
(29)

In the same way, we can prove the equation 9 for odd subcarriers.

ACKNOWLEDGMENT

This work is supported by the Lebanese University research program.

REFERENCES

- A. Osseiran, F. Boccardi, B. Volker, and others, "Scenarios for 5G mobile and wireless communications: the vision of the METIS project," IEEE Communications Magazine. vol. 52, pp. 26–35,2014.
- [2] D. Gesbert, M. Shafi, and others, "From theory to practice: An overview of MIMO space-time coded wireless systems," IEEE Journal on selected areas in Communications. vol. 21, pp. 281–302,2003.
- [3] C. Shin, R. Heath, and E. Powers, "Blind channel estimation for MIMO-OFDM systems," IEEE Transactions on Vehicular Technology. vol. 56, pp. 670–685,2007.
- [4] YS. Cho, J. Kim, WY.Yang and CG. Kang, "MIMO-OFDM wireless communications with MATLAB," John Wiley & Sons, 2010.
- [5] H. Kaur, M. Khosla, and R. Sarin, "Channel Estimation in MIMO-OFDM System: A Review," 2018 Second International Conference on

- Electronics, Communication and Aerospace Technology (ICECA), pp. 974-980,2018.
- [6] R. Hidayat, AF.Isnawati, F. Anggun and B. Setiyanto, "Channel estimation in MIMO-OFDM spatial multiplexing using Least Square method," Intelligent Signal Processing and Communications Systems (ISPACS), 2011 International Symposium on, IEEE, pp. 1-5,2011.
- [7] E. Larsson and P. Stoica, "Space-time block coding for wireless communications," Cambridge university press, 2008.
 [8] U. Jha and R. Prasad, "OFDM towards fixed and mobile broadband wireless access," Artech House, Inc., 2007.
- [9] A. Beydoun, H. Alaeddine and others, "New fast time synchronization method for MIMO-OFDM systems," 11th IFIP Wireless and Mobile Networking Conference (WMNC), IEEE, 2018.
- [10] P. Fan and M. Darnell, "Sequence design for communications applications," Research Studies Press, 1996.
- [11] A. Shokair, A. Beydoun, D.G. Pham and C. Jabbour, "Wide band digital predistortion using iterative feedback decomposition,"Analog Integrated
- Circuits and Signal Processing, pp. 1–16, 2018. [12] B. OHara and A. Petrick, "The IEEE 802.11 Handbook: A Designers Companion," Standards Information Network IEEE Press, 2005.



Ali Beydoun was born in Beirut, Lebanon, in 1980. He received a B.S. in Electronics from the Lebanese University in 2002, an Engineering Degree in Telecommunications from the ENSIETA school, Brest, France, in 2004 and a Ph.D in Electronics from Paris XI university in 2007. From 2007 to 2009, he was a research assistant at the Institut Telecom - ParisTech. Since October 2009, he is professor at the Lebanese university. His research interests include sigma delta modulation, acoustic echo cancellation, timing synchronization

and channel estimation for MIMO OFDM system and digital processing for power amplifier linearization.



Hamz Haidar ALAEDDINE was born in Lebanon, in1980. He received the B.Sc. degree in electronics from the Lebanese University, Lebanon, in 2002, and the M.Sc. degree from University of Brest, France, in 2003. In 2007, he received the Ph.D. degree from University of Brest, France. From 2008 to 2009, he was a Research Scientist with Department of Electrical Engineering, Ecole Polytechnique de Montréal, Canada. He joined in 2010 the Lebanese University. His research interests include Signal Processing for Telecommunications,

adaptive filtering, echo cancellation, number theoretic transform and RF design for wireless systems.